

Kamna Khetarpal¹,
Ritesh Yadav²

Heat Transfer Effects on Non-Newtonian Fluids: Nanofluid Analysis in Helical Heat Exchangers



Abstract: This study investigates the heat transfer characteristics of non-Newtonian nanofluids in a helically baffled heat exchanger with elliptic tubes, combining experimental and numerical approaches. Xanthan gum (XG) aqueous solutions (0.2 wt%) serve as the non-Newtonian base liquid, with multi-walled carbon nanotubes (MWCNTs) dispersed at various weight fractions (0.2%, 0.5%, and 1.0%). Single-phase and multiphase flow models are employed to examine convective heat transfer and fluid flow dynamics in porous media. Results indicate significant enhancement in heat transfer with increasing Reynolds number and nanoparticle concentration. For nanofluids, Nusselt numbers increase by 11% to 35%, and thermal performance factors improve by 3% to 26%. Numerical simulations validate experimental findings, with strong agreement observed. Correlations for predicting Nusselt numbers, friction factors, and Euler numbers are proposed. This research highlights the importance of grid quality in simulations and offers insights into optimizing heat exchanger performance with nanofluids.

Keywords: Non-Newtonian Nanofluids , Multi-Walled Carbon Nanotubes (MWCNTs) , Helically Baffled Heat Exchanger , Convective Heat Transfer, Numerical Simulation, Tortuosity and Hydraulic Conductivity.

I. INTRODUCTION

Heat transfer plays a vital role in numerous industrial and engineering applications, ranging from chemical processing and energy systems to advanced cooling technologies. The development of efficient heat transfer methods is critical for optimizing energy consumption and achieving sustainable solutions. In recent years, the use of non-Newtonian fluids, characterized by their complex flow behavior, has gained attention for heat transfer applications. These fluids, due to their non-linear viscosity profiles, present unique opportunities and challenges in thermal systems. The introduction of nanotechnology, particularly nanofluids, has further revolutionized this field by enhancing the thermal properties of conventional fluids. This study focuses on understanding the heat transfer effects of non-Newtonian fluids, specifically xanthan gum (XG) aqueous solutions, combined with multi-walled carbon nanotubes (MWCNTs), in helically baffled heat exchangers.

Non-Newtonian fluids, unlike Newtonian fluids, exhibit a viscosity that varies with the rate of shear strain. This characteristic makes them highly suitable for specialized applications requiring tailored flow and thermal properties. Xanthan gum (XG), a biopolymer, is a commonly used non-Newtonian fluid due to its stability, biodegradability, and thickening properties. Its applications span across industries such as food processing, pharmaceuticals, and oil recovery. However, its heat transfer efficiency in thermal systems can be limited by its inherent properties. To overcome this limitation, the incorporation of nanoparticles, like MWCNTs, into the base fluid has emerged as a promising solution. MWCNTs are known for their exceptional thermal conductivity, high aspect ratio, and stability, making them an ideal additive to enhance the thermal performance of XG-based fluids.

Heat exchangers, as essential components of thermal systems, play a crucial role in transferring heat between fluids efficiently. Helically baffled heat exchangers, in particular, are designed to induce a swirling flow, which improves heat transfer by reducing boundary layer thickness and enhancing turbulence. The combination of non-Newtonian nanofluids and helically baffled heat exchangers creates a synergistic effect that significantly enhances heat transfer performance. The complex interaction between fluid dynamics and thermal properties in these systems necessitates detailed experimental and numerical investigations to optimize their design and operation.

In this study, xanthan gum aqueous solutions were used as the base fluid, with MWCNTs dispersed at various weight fractions to create non-Newtonian nanofluids. Experimental and numerical analyses were conducted to investigate the heat transfer effects of these nanofluids in helically baffled heat exchangers with elliptic tubes. The study aimed to evaluate key parameters, such as Nusselt number, friction factor, and comprehensive thermal performance factors, to

^{1,2}Department of Physics

^{1,2}Dr. A. P. J. Abdul Kalam University, Indore, India

Corresponding Author: kanu.khetarpal.kk@gmail.com

determine the extent of heat transfer enhancement. Additionally, correlations for predicting these parameters were developed and validated against experimental results.

The use of numerical simulations, alongside experiments, offers a powerful approach to understanding fluid behavior and heat transfer characteristics. Advanced computational tools allow for the detailed analysis of flow pathways, tortuosity, and hydraulic conductivity, particularly in porous media. This study utilized numerical grids generated from 2D reconstructions of Berea sandstone to further explore single-phase and multiphase flow dynamics. These simulations provided insights into the impact of grid quality and resolution on thermal and hydraulic properties, highlighting the critical role of visualization and preprocessing tools in achieving accurate results.

The findings of this research have significant implications for the design and optimization of thermal systems utilizing non-Newtonian nanofluids. By demonstrating the enhanced heat transfer capabilities of XG-MWCNT nanofluids, this study contributes to the growing body of knowledge on advanced heat transfer fluids. The proposed correlations and numerical methodologies offer a practical framework for engineers and researchers to design more efficient and reliable heat exchangers. Furthermore, the results emphasize the importance of integrating experimental and computational approaches to address the challenges of complex fluid systems.

II. LITERATURE REVIEW

Work on vortices between concentric rotating cylinders is the most well-known contribution and concept in the field of fluid dynamics. Indeed, this was a collaborative effort in which theory and experiment were matched at the same time. It is worth noting that a more abstract study that indicates the potential of resistive instability. Convection and flow between revolving cylinders were both shown mathematically, demonstrating that they are mathematically equivalent issues. In reality, it was the use of more recent mathematical concepts that was the key to Tollmein's early success, performed more estimates of the critical Reynolds number and amplification rates of disturbances shortly after, following the same track [1].

As part of an endeavour to explain and anticipate the phenomena of stability and instability, a vast body of theoretical work has been generated by researchers including, Early in this century, investigations on hydrodynamic stability were linked to the Bénard experiments on thermal convection in thin liquid layers, which were carried out in the same laboratory. Around 1907, it became apparent that the existence of a critical Reynolds number could not be easily explained, and that the problem involved both the effects of the second derivative of the mean flow and the effects of viscous forces. For twenty-two years, the Orr-Sommerfeld problem remained unsolvable until the first neutral eigenvalues and determined a crucial Reynolds number for the system of equations. Developed a better mathematical approach that not only resolved the contentious question of the stability of Poiseuille flows, but also set the groundwork for the broad development of the stability analysis in the following decades. Any remaining uncertainties about this system were ultimately dispelled by the first application of a digital computer in hydrodynamical stability calculations [2]. As a consequence of this achievement and the experimental results, it became crystal evident that the critical Reynolds number represented merely the threshold of 'sinuous movement.' It did NOT represent the threshold of turbulence. And the tumultuous changeover has remained an engima for now [3].

fluid is a constantly deforming material that is subjected to the action of applied shear stress. A fluid's flow can have many different characteristics, such as being uniform or non-uniform, compressible or incompressible, viscous or inviscid, rotating or irrotating, steady or unstable, and so on. A boundary layer is a narrow area of fluid flow in which the flow is impacted by the friction between a solid surface and the fluid in which the fluid is flowing. A great deal has been written on the flow of boundary layers in the literature, and they play an important role in the study of fluid dynamics. Boundary layer flows across a horizontal surface have a plethora of industrial uses, including food manufacture, the creation of glass fibres, and the fabrication of rubber sheets, extrusion, metal spinning, wire drawing, and the cooling of large metallic plates, such as electrolytes [4]. Credited with being the first to introduce the theory of the boundary layer [5]. In their paper, presented the numerical computations for the boundary layer flow model due to a stretching sheet with variable electrical conductivity and variable viscosity, which were carried out using the shooting technique in conjunction with a sixth order RK integration algorithm [6]. They came to the conclusion that increasing the electrical conductivity parameter causes a drop in the rate of convective heat transfer and a decrease in the skin friction coefficient within the boundary surface. A further consequence of an increase in the variable viscosity

parameter is a corresponding increase in viscous force, which makes viscous forces more powerful than the applied magnetic field [7]. With the use of the numerical shooting approach, investigated the boundary layer flow through a vertically moving flat sheet with Joule heating and chemical reaction effects [8]. A series of studies investigated the fluid flow and thermal boundary layer travelling over a flat sheet in greater depth than previously reported. A variety of geometries with permeable boundary surfaces were investigated to determine the effect of viscous dissipation and Newtonian heating on fluid flow in the presence of permeable boundary surfaces [9]. In particular, they want to look at mathematical models of Newtonian and non-Newtonian fluid flow across a stretched surface. Describe some of the most notable research on boundary layer fluid flow past a stretched sheet that have been conducted.

Heat transfer is the flow of thermal energy from one system to another as a result of temperature differences between the systems. Because of the difference in temperature between two bodies or between two bodies that are comparable, the phenomenon of heat transfer occurs. In numerous industrial developments, such as the manufacturing of composite materials, geothermal reservoirs, drying of porous solids, thermal insulation, oil recovery, and underground species transport, the investigation of fluid flow and heat transfer generated by means of stretching medium is extremely important. In the examples above, heat transfer and flow investigation are of critical relevance since the ultimate product quality is governed by the coefficient of velocity gradient skin friction and the rate of convective heat exchange, both of which are dependent on the skin friction coefficient. With the assumption that the stretched sheet is exponentially continuous [10], numerically investigated the flow of viscous fluid as well as heat transfer. According to his study, a fluid occupies the space across an infinite horizontal surface, and the flow is caused by the surface's non-linear stretching and deformation. The modelled equations are solved using a numerical approach in this case. The results showed that increasing the suction parameter's value may be utilised to cool the continuous moving stretching surface, and that increasing the suction parameter's value can minimise the thickening level of the thermal boundary layer [11]. As a result, expanded the work of to include heat and mass transfer of a second order viscoelastic fluid across an exponentially extending surface, which was previously only considered. The consequences of elastic deformation and viscous dissipation are among the topics covered in their research. The key result reached by the authors was that when the local viscoelastic parameter increases, the velocity gradient and convective heat exchange Nusselt number decrease at the boundary surface, which is consistent with previous findings [12]. Produced computational conclusions for the mass and transport of viscous fluid caused by a stretched sheet, which were then validated experimentally. It is advised that readers read In order to have a better understanding of boundary layer fluid flow and heat transfer properties over a moving surface [13].

III. EXPERIMENTAL METHOD

3.1 Sample Preparation and Measurements

A homogeneous dispersion of XG was obtained by dissolving the compound in deionized water for roughly an hour with ultrasonic vibration, resulting in aqueous solutions with 0.2 percent weight fraction of XG. A non-Newtonian nanofluid containing MWCNTs was created by mixing aqueous solutions of XG with the suspension of MWCNTs [14]. A series of non-Newtonian nanofluids with MWCNT concentrations of 0.2%, 0.5 wt%, and 1% were created to study how the MWCNT concentration affects the flow and heat transfer properties of the nanofluids [15].

The rotating rheometer (TA-Instrument. Inc., ARG2, New Castle, DE, USA) was used to assess the rheological properties of the base fluid and the non-Newtonian nanofluids with an accuracy of 5 percent [16]. To determine the thermal conductivity and specific heat of the sample, we used a thermal constant analyzer (TPS2500; Hot Disk Company Limited; Uppsala, Sweden) and a DSC (Q20; TA Instruments Company Limited; New Castle, Delaware; USA). TPS2500 and Q20 have recorded accuracies of 3 percent and 5 percent, respectively [17]. An instrument called a densitometer is used to measure the density of samples with an accuracy of less than 0.0001 g/cm³. For all of the measurements, we used a constant temperature bath that was capable of maintaining temperature homogeneity within 0.1 °C in a range of 25 to 65 degrees Celsius. An average value was computed from the results of at least three measurements made at each temperature.

3.2 Experimental System

Experiments to investigate non-Newtonian nanofluids flowing through the shell side of the heat exchanger of the kind described in He, Z.B. et. al., (2016)¹ were carried out using the identical experimental equipment as depicted in Figure

1. Non-Newtonian nanofluid loop, coolant (water) loop, and data gathering system are the three components of the system. Preheaters are used in the non-Newtonian nanofluid loop to heat the non-Newtonian nanofluid prior to cooling it in the heat exchanger. Following heat exchange using a non-Newtonian nanofluid, a cooling tower is used to chill hot water from the tested heat exchanger [18]. contains all the information on the experiment [19]. Measurement errors are provided in this study since they vary somewhat depending on the fluid tested, even if the same equipment is used. Shell side non-Newtonian nanofluid flow rates varied from 1.2 to 1.8 $M^3.h^{-1}$ while shell side non-Newtonian nanofluid flow rates ranged from 1.3 to 1.9 $m.s^{-1}$ at the highest velocity. Shell and tube heat exchangers were often limited to a maximum velocity of less than 2.0 $m.s^{-1}$ for high viscosity fluids due to pressure drop restrictions [20]. It was necessary to maintain a consistent water coolant flow rate in the tube at a value of 1.95 $M^3.h^{-1}$. Here 65 ± 0.1 °C was the intake temperature for non-Newtonian nanofluids [21]. The water coolant's input temperature was maintained at 30 ± 0.1 C. Agilent 34970A data system records temperature and pressure (Santa Clara, CA, USA). During the 15-minute scan period, the application was set to run 10 times for each data point. Analytically, all of the measurements were averaged.

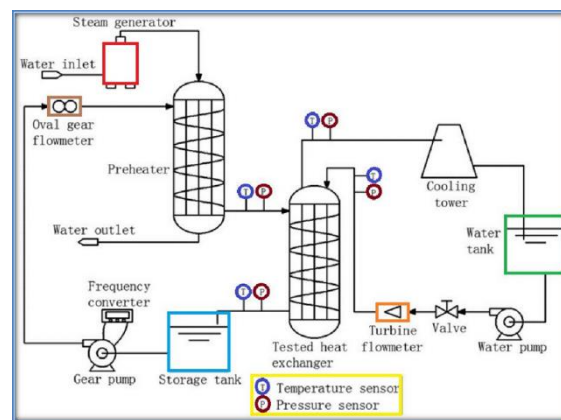


Figure 1: Heat transfer experiment set-up schematic diagram.

V. SIMULATION SPECIFICS

OpenFOAM, a free and open source CFD software programme developed by OpenCFD Ltd, was utilised for the current investigation. OpenFOAM is a free and open source CFD software product. Simulations have been carried out for both single-phase flow (water injection through a 2D geometry Fig (4.1)) and two-phaseflow (oil drainage by water injection Fig (4.3)). We wanted to see how the image reconstruction process and grid quality affected our estimates of flow through a certain porous material, so we looked into it. The classic laminar Navier- Stokes equations of mass and momentum conservation were used in the single-phase simulations. The standard Volume of fluid method (VOF) (Georgoulas A, et al., 2015)⁶ is used to model multiphase flows in this study. This approach follows the interface between the two fluids, and an additional term accounting for surface tension forces between the two liquids has been added to the momentum equation to account for the surface tension forces between the two fluids. It is believed that the fluids used in both single-phase and multiphase runs are both incompressible and indestructible. The flow is isothermal in nature. Listed here are some of the physical characteristics of water and oil, along with their respective inlet conditions (4.1).

Table 1: The qualities of the fluid and the preliminary circumstances

Parameter	Symbol (units)	Value
Volumetric flow rate (single phase)	Q (m^3/s)	8.333e-11
Volumetric flowrate (two-phase)	Q (m^3/s)	1e-10
fluid density(water)	ρ (kg/m^3)	998
fluid dynamic viscosity (water)	μ (Ns/m^2)	8.88e-4
fluid density (oil)	ρ (kg/m^3)	835
fluid dynamic viscosity (oil)	μ (Ns/m^2)	0.1
Surface tension(water to oil)	N/m	0.048
Contact angle at the triple line	degrees	45

5.1 Thermal-Physical Properties of Non-Newtonian Nanofluids

Figure 2 shows the variation of the viscosity η of base fluid and nanofluids with the shear rate $\dot{\gamma}$ at 25°C. As can be seen from Figure 2, the viscosities of all working fluids decreases with the increasing of the shear rate, indicating

that all these samples are typical non-Newtonian fluids with shear thinning behavior ($n < 1$). For a given shear rate $\dot{\gamma}$, the viscosity increases slightly with the increase in weight fraction of nanoparticle

Thermal-physical properties of base fluid and non-Newtonian nanofluids including consistency index K , power law index n , thermal conductivity λ , density ρ and specific heat c_p were measured and their correlations to temperature are provided in Table 2.

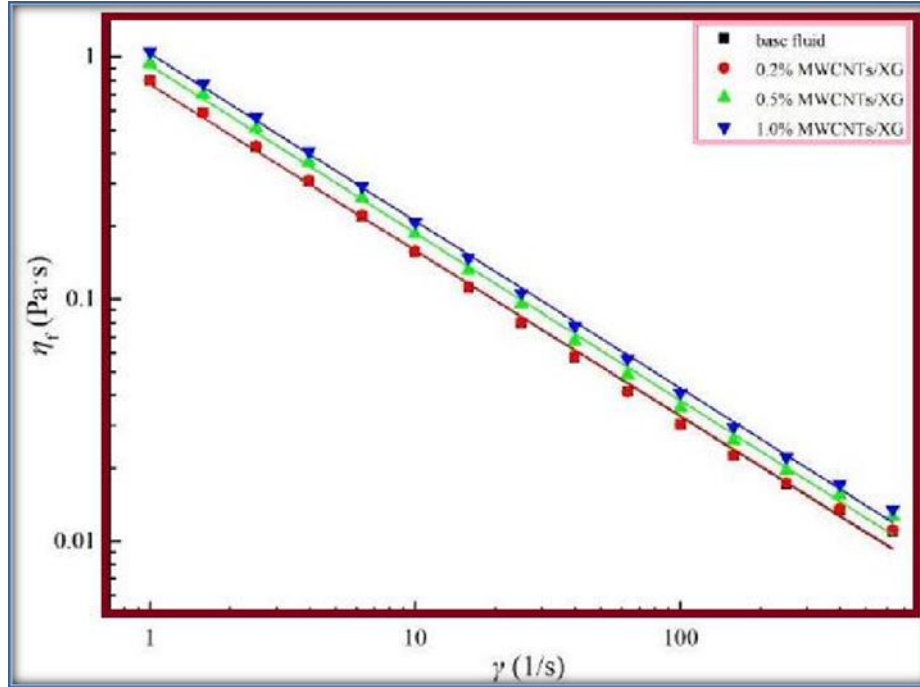


Figure 2: Variation of the viscosity with the shear rate at different concentrations at 20°C.

Table 2: Expression of thermal-physical properties.

Fluid	Correlations (298.15 K < T < 338.15 K)				
	K ($\text{m}^2 \cdot \text{s}^n$)	n	λ ($\text{W} \cdot \text{m}^{-1} \cdot \text{K}^{-1}$)	ρ ($\text{kg} \cdot \text{m}^{-3}$)	c_p ($\text{kJ} \cdot \text{kg}^{-1} \cdot \text{K}^{-1}$)
Base fluid	$-0.0131T + 4.6322$ ($R^2 = 0.999$)	$0.0043T - 0.9469$ ($R^2 = 0.988$)	$0.0043T - 0.6265$ ($R^2 = 0.979$)	$-0.0073T^2 + 4.2840T + 382.8$ ($R^2 = 0.991$)	$-2.7149 \times 10^{-5}T^2 - 0.01189T + 4.8763$ ($R^2 = 0.996$)
0.2 wt % MWCNTs/XG	$-0.0124T + 4.4211$ ($R^2 = 0.999$)	$0.0040T - 0.8517$ ($R^2 = 0.989$)	$0.0035T - 0.4168$ ($R^2 = 0.987$)	$-0.0067T^2 + 3.8902T + 451.2$ ($R^2 = 0.991$)	$-5.4948 \times 10^{-5}T^2 + 0.04071T - 3.5919$ ($R^2 = 0.991$)
0.5 wt % MWCNTs/XG	$-0.0111T + 4.1513$ ($R^2 = 0.992$)	$0.0025T - 0.3962$ ($R^2 = 0.982$)	$0.0026T - 0.1468$ ($R^2 = 0.995$)	$-0.0052T^2 + 2.9004T + 611.5$ ($R^2 = 0.990$)	$-3.9137 \times 10^{-5}T^2 + 0.03135T - 2.3183$ ($R^2 = 0.998$)
1.0 wt % MWCNTs/XG	$-0.0130T + 4.8356$ ($R^2 = 0.996$)	$0.0021T - 0.3016$ ($R^2 = 0.998$)	$0.0025T - 0.1473$ ($R^2 = 0.988$)	$-0.0016T^2 + 0.6362T + 965.2$ ($R^2 = 0.987$)	$6.9542 \times 10^{-5}T^2 - 0.04154T + 9.6727$ ($R^2 = 0.972$)

5.2 Inclusive Performance

Considering both heat transfer performance and flow resistance characteristic, the comprehensive thermal performance factor (TPF) is adopted to evaluate the heat exchanger.

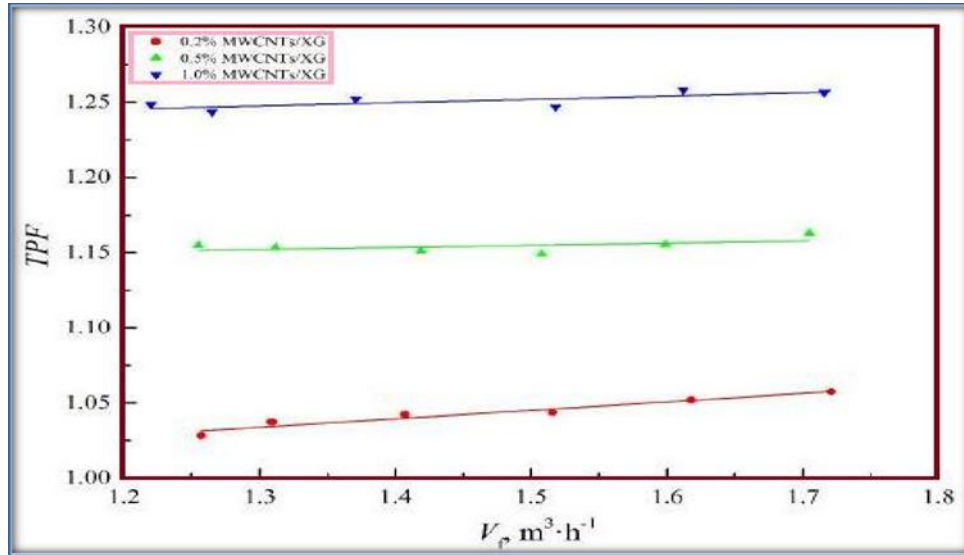


Figure 3. Comprehensive thermal performance factor versus volume flow rate.

5.3 Euler Number

Figure 4. shows the variation of Euler number Eu_o with Reynolds number Re_o in double logarithm coordinate. As shown in Figure 4, Eu_o decreases with the increasing in Re_o and the decreasing in nanoparticle weight fraction. For a given Re_o , the Eu_o of nanofluids at weight fraction of 1.0 wt %, 0.5 wt%, and 0.2 wt% increases by 16%, 7.6% and 3.1% in comparison with base fluid, respectively.

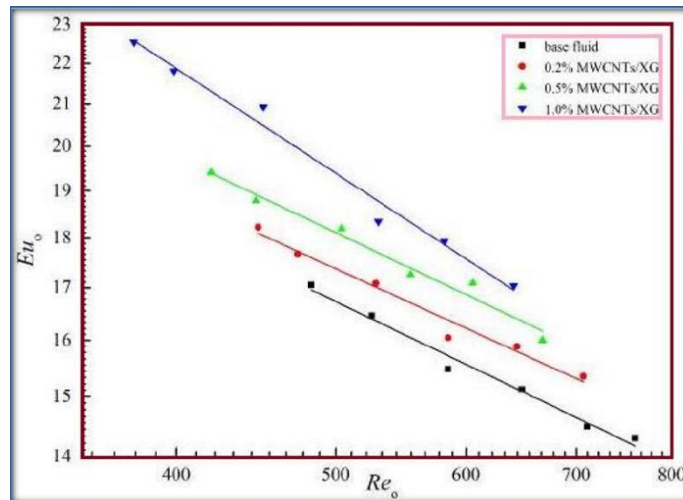


Figure 4: Euler number versus Reynolds number.

5.4 Nusselt Number and Friction Factor

Based on experimental and numerical results, Figures 5 and 6 show the variation of the shell-side Nusselt number Nu_o and friction factor f_o with the Reynolds number Re_o for the base fluid and nanofluids at different concentrations,

respectively. From Figure 5.5, it is found that Nu_o increases with the increasing of

Re_o . For a given Re_o , Nu_o increases with an increasing in the MWCNTs concentration. Based on experimental data, the Nu_o of the non-Newtonian nanofluids at weight fraction of 1.0 wt%, 0.5wt%, and 0.2wt% increases by 35%, 21% and 11% on average while compared with that of the base fluid at the same Reynolds number Re_o , respectively. It can be observed from Figure 5.6 that the experimental f_o of the nanofluids are larger than that of the base fluid, and gradually increases with increasing in the weight fraction of nanoparticles and rapidly decreases with an increase in Re_o . Higher friction factor leads to greater pressure drop in shell side, which is the obvious drawback of nanofluid. The enhanced thermal conductivity and viscosity of nanofluid after adding MWCNTs are response for the increasing of Nu_o and f_o , respectively.

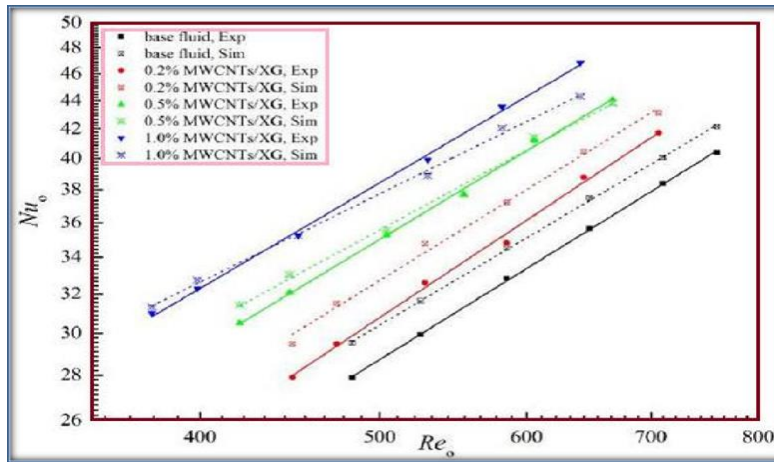


Figure 5: Nusselt number based on experiment and simulation versus shell-side Reynolds number.

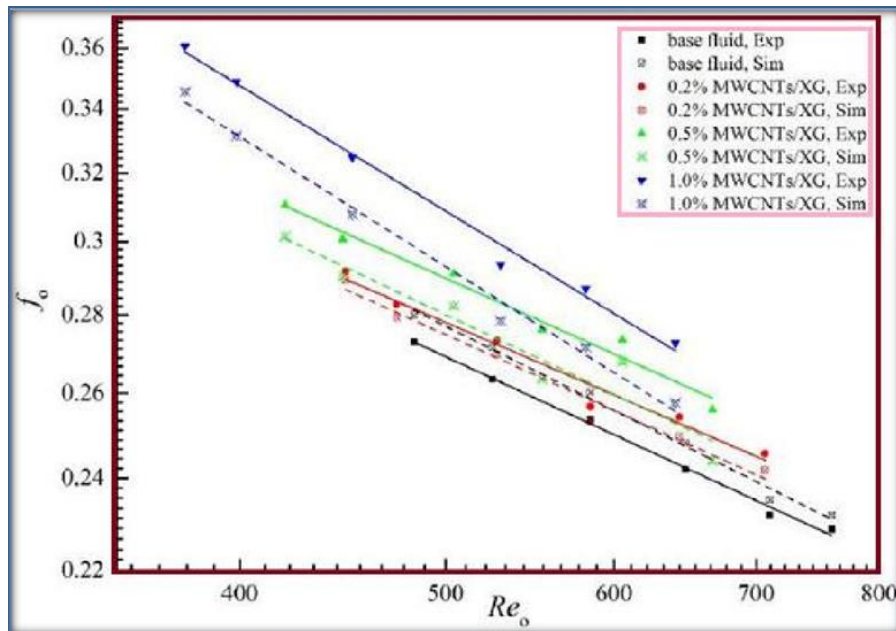


Figure 6: Friction factor based on experiment and simulation versus shell-side Reynolds number.

VI. CONCLUSION

This study employed a single-phase flow model to investigate the convective heat transfer characteristics of non-Newtonian nanofluids in the shell side of a helically baffled heat exchanger with elliptic tubes. Using laminar, single-phase, and two-phase flow simulations at the pore scale (500×500 microns), the research provided insights into optimal flow pathways, tortuosity, and hydraulic conductivity. Numerical simulations were supported by high-quality grid creation and refinement using ANSA, which proved critical in ensuring accuracy and reliability. Initial validation of numerical tools against conventional porous grain configurations from the literature demonstrated their robustness and set the stage for exploring more complex geometries, such as Berea sandstone, characterized by intricate internal structures with sharp-edged grains.

The findings underline the importance of high-resolution grid reconstruction and scale resolution for accurate hydraulic conductivity predictions. While traditional Darcy-based formulas are grid-dependent and may lead to inaccuracies, the study proposes using tortuosity as a grid-independent metric for permeability estimation. The grid's influence extends to multiphase flow simulations, where poor grid quality results in interphase diffusion, erroneous propagation velocities, and missed transitions from viscous displacement to fingering effects.

Future advancements will focus on analyzing increasingly smaller samples to enable the study of larger systems with improved resolution. This integration of micro and macro scales in multiphase flow analysis will facilitate a more comprehensive understanding of flow dynamics, paving the way for optimized heat exchanger designs and enhanced thermal performance in applications involving non-Newtonian nanofluids.

References

- [1] Taylor, Geoffrey I., "Stability of a viscous liquid contained between two rotating cylinders". Philosophical Transactions of the Royal Society of London. Series A, Containing Papers of a Mathematical or Physical Character. Vol. 223, No.14, pp. 605–615, 1923.
- [2] <https://www.encyclopedia.com/education/news-wires-white-papers-and-books/shaye-lin-1944>
- [3] G. B. Schubauer and H. K. Skramstad, "Laminar Boundary-Layer Oscillations and Stability of Laminar flow," Journal of the Aeronautical Sciences, Vol. 14, No. 2, pp. 69-78, 1947.
- [4] Hossein and A. Makhlof, "Industrial applications for intelligent polymers and coatings," Springer, International Publishing, Edition 1, Switzerland, pp. 206-209, 2016.
- [5] L. Prandtl, "On fluid motions with very small friction," International Mathematics Kongr Heidelberg, Auch, vol. 6, No. 1, pp. 484–491, 1904.
- [6] O. Makinde and O. Onyejekwe, "A numerical study of MHD generalized Couette flow and heat transfer with variable viscosity and electrical conductivity," Journal of Magnetism and Magnetic Materials, Vol. 323, No. 2, pp. 2757–2763, 2011.
- [7] S. Ibrahim and O. Makinde, "Chemically reacting magnetohydrodynamics MHD boundary layer flow of heat and mass transfer past a low-heat-resistant sheet moving vertically downwards," Scientific Research and Essays, Vol. 22, No. 1, pp. 4762–4775, 2011.
- [8] S. Liao, "On the analytic solution of magnetohydrodynamic flows of nonNewtonian fluids over a stretching sheet," Journal of fluid Mechanics, Vol. 488, No. 2, pp. 189–212, 2003.
- [9] R. Kumar, G. Kumar, C. Raju, S. Shehzad, and S. Varma, "Analysis of arrhenius activation energy in magnetohydrodynamic Carreau fluid flow through improved theory of heat diffusion and binary chemical reaction," Journal of Physics Communications, Vol. 2, No. 3, pp. 26-36, 2018.
- [10] E. Elbashbeshy, "Heat transfer over an exponentially stretching continuous surface with suction," Archives of Mechanics, Vol. 53, No. 2, pp. 643–651, 2001.
- [11] E. Sanjayanand and K. Khan, "On heat and mass transfer in a viscoelastic boundary layer flow over an exponentially stretching sheet," International Journal of Thermal Sciences, vol. 45, No. 4, pp. 819–828, 2006.
- [12] E. Magyari and B. Keller, "Heat and mass transfer in the boundary layer on an exponentially stretching continuous

- surface,” *Journal of Physics*, Vol. 32, No. 1, pp. 577–585, 1999.
- [13] A. Majeed, A. Zeeshan, S. Almari, and R. Ellahi, “Heat transfer analysis in ferromagnetic viscoelastic fluid flow over a stretching sheet with suction,” *Neural Computing and Applications*, Vol. 6, No. 5, pp. 1947–1955, 2018.
- [14] He, Z.B.; Fang, X.M.; Zhang, Z.G.; Gao, X.N. Numerical investigation on performance comparison of non-Newtonian fluid flow in vertical heat exchangers combined helical baffle with elliptic and circular tubes. *Appl. Therm. Eng.*, Vol. 100, No. 6, pp. 84–97, 2016.
- [15] Kline, S.J.; McClintock, F.A. "Describing uncertainties in single-sample experiments," *Journal of Mech. Eng.*, Vol. 75, No. 9, pp. 3–8, 1953.
- [16] Shih, T.H.; Liou, W.W.; Shabbir, A.; Yang, Z.; Zhu, J. A new $k-\epsilon$ eddy viscosity model for high reynolds number turbulent flows. *Comput. fluids*, Vol. 24, No. 3, pp. 227–238, 1995.
- [17] Dong, C.; Chen, Y.P.; Wu, J.F., "flow and heat transfer performances of helical baffle heat exchangers with different baffle configurations," *Journal of Appl. Therm. Eng.*, Vol. 80, No. 6, pp. 328–338, 2015.
- [18] Tao, W.Q., "Numerical Heat Transfer," 5th Edition, Jiaotong University Press: Xi'an, China, pp. 126-136, 2001.
- [19] Øren P al-E, Bakke S., "Process based reconstruction of sandstones and prediction of transport properties," *Transp Porous Media*, Vol. 46, No. 3, pp. 311–343, 2002.
- [20] Keller AA, Blunt MJ, Roberts APV., "Micromodel Observation of the Role of Oil Layers in Three-Phase flow," *Transp Porous Media*, Vol. 26, No. 3, pp. 277–297, 1997.
- [21] Xiao Z, Yang D, Yuan Y, Yang B, Liu X., "Fractal pore network simulation on the drying of porous media," *Dry Technol*, Vol. 26, No. 6, pp. 651–665, 2008.